

MAUCell: An Adaptive Multi-Attention Framework for Video Frame Prediction

Shreyam Gupta^{*1}, Pranjal Agrawal² and Priyam Gupta³

¹Indian Institute of Technology (BHU), Varanasi, India

²University of Colorado, Boulder, USA

³Intelligent Field Robotic Systems (IFROS), University of Girona, Spain

*shreyam.gupta.mec21@iitbhu.ac.in, u1999097@campus.udg.edu

Abstract

Temporal sequence modeling stands as the fundamental foundation for video prediction systems and real-time forecasting operations as well as anomaly detection applications. The achievement of accurate predictions through efficient resource consumption remains an ongoing issue in contemporary temporal sequence modeling. We introduce the Multi-Attention Unit (MAUCell) which combines Generative Adversarial Networks (GANs) and spatio-temporal attention mechanisms to improve video frame prediction capabilities. Our approach implements three types of attention models to capture intricate motion sequences. A dynamic combination of these attention outputs allows the model to reach both advanced decision accuracy along with superior quality while remaining computationally efficient. The integration of GAN elements makes generated frames appear more true to life therefore the framework creates output sequences which mimic real-world footage. The new design system maintains equilibrium between temporal continuity and spatial accuracy to deliver reliable video prediction. Through a comprehensive evaluation methodology which merged the perceptual LPIPS measurement together with classic tests MSE, MAE, SSIM and PSNR exhibited enhancing capabilities than contemporary approaches based on direct benchmark tests of Moving MNIST, KTH Action, and CASIA-B (Preprocessed) datasets. Our examination indicates that MAUCell shows promise for operational time requirements. The research findings demonstrate how GANs work best with attention mechanisms to create better applications for predicting video sequences.

1 Introduction

The fundamental video frame prediction task of computer vision finds broad practical applications across video compression and surveillance and medical imaging and autonomous systems. The framework demands models to guess future

video frames by processing past inputs and to detect patterns in video spatial arrangement while managing temporal changes. It becomes particularly difficult to achieve precise projections despite maintaining reliable processing speed when performing calculations on intricate motion sequences under fast-paced requirements. Video frame prediction using Recurrent Neural Networks (RNNs) [Wang *et al.*, 2018; Wang *et al.*, 2017] and Long Short-Term Memory (LSTM) [Wang *et al.*, 2019; Srivastava *et al.*, 2016; Villegas *et al.*, 2019] networks faces two challenges: it struggles with maintaining long-term memory dependencies effectively while failing to simultaneously understand spatial and temporal relationships. The new paradigm of generative adversarial networks (GANs) [Lee *et al.*, 2018; Kwon and Park, 2019] enhances perceptual realism yet further research is needed to integrate attention methods [Chang *et al.*, 2022] which refine both spatial and temporal aspects.

This research proposes a new video frame prediction framework through Multi-Attention Unit Cell (MAUCell) architecture. The proposed system incorporates GAN-based adversarial training with spatio-temporal attention mechanisms [Chang *et al.*, 2022] to ensure real-time motion dynamics detection while retaining fine structural information [Akan *et al.*, 2021]. Through a framework known as MAUCell the architecture employs three distinct types of attention mechanisms to focus meaningful processing on essential features thus combining precision with visual fidelity. We make the following contributions through our research:

- Through the use of Multi-Attention Unit Cells we develop a single architectural framework to analyze both temporal and spatial connections while refining output pixels for modeling video sequence dynamics.
- Through integration of Generative Adversarial Network components our framework improves the perceptual quality of predictions by generating outputs which replicates real-world video content.
- We apply our model to benchmark datasets Moving MNIST [Deng, 2012; Lee *et al.*, 2019], KTH Action [Schuldt *et al.*, 2004] along with CASIA-B [Castro *et al.*, 2016; Yee Andres,] and establish superior performance against existing methods by applying MSE, SSIM, PSNR and LPIPS metrics.
- The designed computational framework reaches its de-

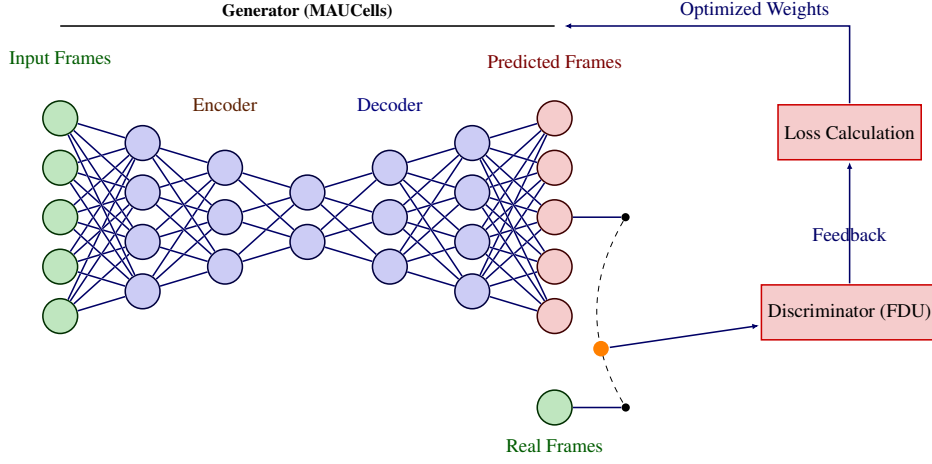


Figure 1: Structure of the proposed GAN based system.

signed speed performance level that enables real-time operations in settings where resources are limited.

2 Model Architecture

A new model structure combines dual components which excel at capturing videos' temporal and spatial dynamics. The model creates video frame predictions at the Generator (G) level through Multi-Attention Units (MAUCells), and the Discriminator (D) validates frame quality to enhance prediction accuracy through adversarial training. A loss calculation model contains integrated optimization metrics as illustrated by the figure 1 adapted from [Izaak Neutelings, ; Riebesell and Bringuier, 2022] .

The architecture comprises two primary components: the Generator and the Discriminator.

2.1 Multi-Attention Unit (MAU) Cell

At the core of the model is the MAUCell, a specialized unit that integrates multiple attention mechanisms to process both temporal and spatial aspects of video frames:

Temporal Attention The learning of temporal attention processes delayed information relationships through frame-by-frame sequence comparison. The framework comprises processing units which examine visual formations between consecutive frames to find and rank fundamental motion tracks and developing environment components. By implementing this technique the model maintains accurate time-dependent relationship awareness throughout the video sequence while efficiently filtering out uninformative or repetitive temporal patterns. Partitioned temporal tendencies undergo modification by adaptive gating functions that regulate historical sequences relative to present data input.

Spatial Attention The model's spatial attention abilities allow proper detection and storage of local and global spatial elements found inside video frames. Layered algorithms within the system examine frame pixels and their spatial connections to extract valuable spatial information. The model identifies

fundamental structural features consisting of edges and textures and patterns to prioritize essential regions for upholding frame coherency. Force-directed spatial attention mechanisms operate to suppress useless image areas while enabling a more focused allocation of processing power toward the portions that significantly enhance prediction accuracy. The combined framework maintains optimal resolution alongside structural consistency because this method protects important details needed for accurate video generation.

Algorithm 1 Multi-Attention Unit Cell (MAUCell)

- Require:** Video frames T_t, S_t , Attention weights $t_att, s_att, s_pixel_att$
- Ensure:** Updated attention outputs out_T, out_S
- 1: Initialize model parameters α_s, α_t and hidden dimensions Θ
 - 2: Compute temporal and spatial attention projections:
 - 3: $s_next = \text{Conv}(S_t), t_next = \text{Conv}(T_t)$
 - 4: Aggregate temporal trends: $T_trend = \sum_{i=1}^{\tau} \text{Softmax}\left(\frac{s_att[i] \cdot s_next}{\sqrt{d}}\right) \cdot t_att[i]$
 - 5: Compute gating mechanisms:
 - 6: $t_att_gate = \text{Sigmoid}(t_next), s_att_gate = \text{Sigmoid}(s_next)$
 - 7: Fuse features:
 - 8: $T_fusion = T_t \cdot t_att_gate + (1 - t_att_gate) \cdot T_trend$
 - 9: $S_fusion = S_t \cdot \text{Sigmoid}(s_pixel_att)$
 - 10: Split and apply activations:
 - 11: $t_i, t_r, t_t, t_s = \text{Split}(\text{Conv}(T_fusion))$
 - 12: $s_i, s_r, s_t, s_s = \text{Split}(\text{Conv}(S_fusion))$
 - 13: Compute updated features:
 - 14: $T_new_1 = T_r \cdot T_i + S_t \cdot T_fusion$
 - 15: $S_new_1 = S_r \cdot S_i + T_s \cdot S_fusion$
 - 16: Apply weighted fusion:
 - 17: $out_T = \alpha_t \cdot T_new_1 + (1 - \alpha_t) \cdot T_new_2$
 - 18: $out_S = \alpha_s \cdot S_new_1 + (1 - \alpha_s) \cdot S_new_2$
 - 19: **return** out_T, out_S
-

Pixel Attention Pixel-wise attention works by focusing on specific frame regions that demonstrate crucial connection to prediction requirements at pixel scale. The method evaluates localized importance through pixel-by-pixel investigations of intensity variations and structural patterns which enables strong emphasis of critical features needed for precise predictions.

Fusion Mechanisms As a part of its functionality the MAUCell merges attention outputs by using two separate integration methods. The Temporal Fusion algorithm unifies motion data by merging historical patterns with active temporal characteristics. The model obtains the ability to maintain equilibrium between short-term and extended temporal information. Through Spatial Fusion the model combines pixel-based attention outputs with spatially important regions to understand the frame’s spatial organization. The processing system guarantees that all produced images maintain their structural design along with their visual accuracy. Unlike existing methods [Chang *et al.*, 2021] that merges only movement data from the temporal state while gathering aspect information from the spatial state.

Learnable Parameters The MAUCell introduces learnable parameters and to dynamically adjust the weighting of temporal and spatial fusion outputs. Through learnable parameters the model can achieve optimal temporal coherence and spatial consistency adjustment in response to different input requirements.

2.2 Recurrent Neural Network Backbone

The system architecture implements a multi-layer RNN design which utilizes MAUCell stacks to process sequential information sequencing. Key aspects include:

- Encoding Layers: The extraction process uses sequential downsampled convolutional layers which develop detailed spatial information across different scales.
- Decoding Layers: The model constructs detailed high-resolution pictures through transposed convolutions together with skipping structures that sustain fundamental spatial data.
- Temporal Window: Through the temporal attention window setting the model can use a specified number of accessible historical frames helping it detect extended time-span connections in the input data.

2.3 Discriminator Module

An essential component of the generator is the Frame Discriminator Unit (FDU) which assesses predicted frame quality to support generator output refinement. As an adversarial component the module returns corrective data which optimizes the generator output. The discriminator establishes frame quality assessment by learning to distinguish real frames from those produced by the generator while maintaining temporal consistency and structural accuracy. Through multi-scale extraction the discriminator evaluates basic and advanced frame features which leads to improved generated frame realism.

Algorithm 2 MAU-Based Sequential Video Prediction Framework

Require: Input frames $X = \{x_1, x_2, \dots, x_T\}$, Ground-truth mask Mask_true , Model parameters Θ (encoders, decoders, MAUCells)

Ensure: Predicted frames $\hat{X} = \{\hat{x}_{T+1}, \dots, \hat{x}_{T+H}\}$
 1: Initialize temporal and spatial features $T_t, T_{\text{pre}}, S_{\text{pre}}, S_{\text{prev}}$ to zeros

2: **for** $t = 1$ **to** $T + H$ **do**

3: **if** $t \leq T$ **then**

4: Set input frame: $x_t \leftarrow X[t]$

5: **else**

6: Perform scheduled sampling:

$$x_t \leftarrow \text{Mask_true}[t-T] \cdot x_t + (1 - \text{Mask_true}[t-T]) \cdot \hat{x}_t$$

7: **end if**

8: Encode input frame through encoder layers: $S_t \leftarrow \text{Encoders}(x_t)$

9: Compute pixel-level attention:

$$S_{\text{pixel.att}} \leftarrow \|S_t - S_{\text{prev}}\|^2$$

10: Update spatial features: $S_{\text{prev}} \leftarrow S_t$

11: **for each** MAUCell layer i **do**

12: Gather temporal and spatial attention:

$$t_att \leftarrow T_{\text{pre}}[i], s_att \leftarrow S_{\text{pre}}[i]$$

13: Update features using MAUCell:

$$T_t, S_t \leftarrow \text{MAUCell}[i](T_t, S_t, t_att, s_att, S_{\text{pixel.att}})$$

14: Append updated features: $T_{\text{pre}}[i] \leftarrow T_t, S_{\text{pre}}[i] \leftarrow S_t$

15: **end for**

16: Decode spatial features to predict frame:

$$\hat{x}_t \leftarrow \text{Decoders}(S_t)$$

17: Store predicted frame: $\hat{X}[t] \leftarrow \hat{x}_t$

18: **end for**

19: Return all predicted frames: \hat{X}

3 Experiment

3.1 Training Framework

A thorough training system incorporates several loss functions while employing optimization methods together with graphical display components to create effective learning.

Instances of architecture emerge through the specification of adjustable parameters consisting of layers count together with hidden unit number and input dimension details. The factory pattern chooses between different model variants (such as RNN-based generators) and sets each network to use specific device configurations during initialization. During adversarial training the discriminator becomes an equivalent

Algorithm 3 Frame Discriminator Unit (FDU)

Require: Input frames $X = \{x_1, x_2, \dots, x_T\}$ (real or generated), Model parameters Θ (encoders, MAUCells)

Ensure: Discrimination results $Y = \{y_1, y_2, \dots, y_T\}$ (real or fake classification for each frame)

1: Initialize temporal and spatial features $T_t, T_{pre}, S_{pre}, S_{prev}$ as zero tensors

2: **for** $t = 1$ **to** T **do**

3: Extract spatial features S_t using encoder layers:

$$S_t = \text{Encoders}(x_t)$$

4: Compute pixel-level attention for frame S_t :

$$S_{\text{pixel_att}} = \|S_t - S_{\text{prev}}\|^2$$

5: Update spatial features: $S_{\text{prev}} \leftarrow S_t$

6: **for** each MAUCell layer i **do**

7: Gather temporal and spatial attention:

$$t_att \leftarrow T_{\text{pre}}[i], s_att \leftarrow S_{\text{pre}}[i]$$

8: Update features using MAUCell:

$$T_t, S_t = \text{MAUCell}[i](T_t, S_t, t_att, s_att, S_{\text{pixel_att}})$$

9: Append updated features:

$$T_{\text{pre}}[i] \leftarrow T_t, S_{\text{pre}}[i] \leftarrow S_t$$

10: **end for**

11: Compute classification for frame x_t :

$$y_t = \text{Decoder}(S_t, T_t)$$

12: Store classification result: $Y[t] \leftarrow y_t$

13: **end for**

14: **return** Discrimination results Y

network instance to the generator.

Designing prediction quality capture requires the framework to use several loss components simultaneously.

- Mean Squared Error (MSE) Loss: Pixel-level differences between frame predictions and original ground reality structures are measured through this loss function which optimizes structural accuracy.
- L1 Loss: By minimizing absolute deviations and refining precise textural contents the model improves.
- Binary Cross-Entropy (BCE) Loss: When used for adversarial training it determines whether the discriminator can recognize authentic frames from synthetic ones.

The total generator loss L_{gen} is a weighted combination:

$$L_{gen} = \alpha * L_{MSE} + \beta * L_{L1} + \gamma * L_{adv}$$

where α, β, γ are hyperparameters dynamically adjusted during training.

Frame Type	Description
Input Frames	Frames fed into the model as context for prediction.
Ground Truth	Actual frames used for comparison with generated outputs.
Generated Frames	Predicted frames generated by the model.
Attention Masks	Visual representation of regions where the model focuses its attention.

Table 1: The training framework provides periodic plots, helping researchers track the model’s performance qualitatively.

When adversarial training is enabled, the framework employs a Generative Adversarial Network (GAN) paradigm. Discriminator Loss L_{disc} that combines losses from real and generated frames.

$$L_{disc} = BCE(D_{real}, 1) + BCE(D_{fake}, 0)$$

where D_{real} and D_{fake} denote the discriminator’s predictions for real and generated frames, respectively.

Generator Adversarial Loss encourages the generator to produce frames indistinguishable from real frames.

$$L_{adv} = BCE(D_{fake}, 1)$$

The generator and discriminator are optimized using the Adam optimizer with learning rate schedules to adaptively reduce the learning rate after a predefined number of iterations. This ensures stable convergence and prevents overfitting.

The training framework provides periodic plots of input, ground truth, and generated frames, helping researchers track the model’s performance qualitatively.

3.2 Evaluation Methodology

The model leverages three datasets, each targeting distinct challenges in video prediction:

Moving MNIST: The dataset consists of static handwritten digit pairs taken from the MNIST dataset which move continuously across a frame. A total of 7,000 training and 3,000 testing sequences contained digits which moved between static frames and produced edge collisions and channel intersections. All data sequences received a 64×64 pixel format and normalization processing adjusted their range between 0 to 1.

KTH Action The dataset consists of 5,686 training sequences across six human action types performed by 25 individuals in four different settings while using 2,437 sequences as test data. The frames received 64×64 pixel rescaling followed by spatial normalization transformations.

CASIA-B (Preprocessed) This dataset presents gait pattern sequences which were recorded at different views with various environmental conditions related to pedestrian motions. Each data sequence received both size modifications into 64×64 format and normalization treatment. A specific range of camera viewpoints including side views was used for maintaining training consistency.

Metric	Description	Insight Provided
MSE	Measures pixel-wise differences between predicted and ground truth frames.	Lower MSE values indicate better pixel-wise prediction accuracy.
MAE	Captures absolute deviations for texture-level fidelity.	Lower MAE values indicate better pixel-level accuracy.
SSIM	Evaluates perceptual similarity and structural consistency.	Higher SSIM values indicate better structural similarity between predicted and ground truth frames.
PSNR	Quantifies reconstruction quality based on pixel intensity.	Higher PSNR values suggest better visual quality of the predictions.
LPIPS	Measures perceptual similarity using deep feature embeddings.	Lower LPIPS values indicate better perceptual similarity to human perception.

Table 2: Evaluation metrics summary

A dedicated data processing pipeline was developed to execute both preprocessing needs and augmentation requirements. Stable numerical values during training were achieved by normalizing all pixel intensities to occupy the $[0,1][0, 1]$ scale. Image frames underwent a 64×64 resolution change along with essential aspect ratio preservation. The input frames were broken down into multiple smaller segments to better detect localized elements. The TimeSeries-Dataset [Michalski *et al.*, 2014] class structures video sequences through partnerships between input elements and output elements. The initial 10 frames of each sequence offer essential temporal information to the model. The modeled system generates predictions during the next 10 frames.

The model received improved prediction robustness through scheduled sampling implementation. The probabilistic mask system decides between model predictions and ground truth data passed during training sessions. As training continues the probability (η) shows linear reduction.

$$\eta = \max(0, \eta - r * t)$$

where r is the decay rate

The discriminator uses a $2 * 10^{-4}$ learning rate alongside a 0.9 decay factor which adjusts it at 2,000 iterations for network optimization. The generator operates with the same learning rates and decay parameters. We used 16 samples per batch. The model training continues up to 7 epochs or reaches 150,000 iterations.

Our research compared the proposed GAN video frame predictor using attention mechanisms against established state-of-the-art techniques. This study presents a comprehensive evaluation which identifies our approach’s innovative aspects together with existing research limitations while assessing the method’s numerous advantages and potential weaknesses. The proposed model undergoes comparative evaluation against contemporary approaches [Chang *et al.*, 2022; Chang *et al.*, 2021; Denton and Fergus, 2018; Gao *et al.*, 2022; Guen and Thome, 2020; Lee *et al.*, 2018; Lee *et al.*, 2021; Lin *et al.*, 2020; Tang *et al.*, 2023; Wang *et al.*, 2019; Sun *et al.*, 2023; Wang *et al.*, 2017; Wang *et al.*, 2022; Yu *et al.*, 2020; Zhong *et al.*, 2023; Villar-Corrales *et al.*, 2022] across multiple datasets while incorporating multiple quantitative metrics alongside qualitative assessments.

To comprehensively assess the model’s performance, the metrics employed are summarized in the Table 2:

Quantitative results for the MNIST datasets is summarized in the Table 3. Our system demonstrates better performance than current methods by maintaining elevated SSIM and PSNR metrics which indicate outstanding structural preservation alongside exceptional reconstruction quality. The model demonstrates improved SSIM performance because it effectively maintains shape and edge spatial consistency when processing sequences. The embedded spatial temporal attention mechanisms in the MAUCell allow accurate motion detection while preserving digit structure free of smearing effects.

Human perception evaluations from LPIPS values reveal our model’s superiority over its closest competitor STAU through diminished measurement results. Pixel-wise attention mechanisms improve frame generation by focusing on important frame regions and maintaining sequence perceptual coherence.

Our model demonstrates the highest operational speed of 14.1 seconds while outperforming SwinLSTM and all additional models with an evaluation time exceeding 18.1 seconds. The significant reaction time reduction derives from the lightweight MAUCell architecture design that eliminates useless computations while preserving essential model expressiveness. Successful application of attention mechanisms alongside their effective structure enables faster inference operations that maintain real-time capabilities.

Predicting on the Moving MNIST dataset becomes complex because overlapping digits occur simultaneously during training without sacrificing prediction clarity. Our method differs from PhyDNet and other approaches by needing no manually designed physical dynamic separation strategies. Tractable implementation paths can be established while robust motion pattern recognition remains possible due to this methodology.

Our model employs adaptive attention mechanisms to choose relevant areas of interest which constitutes a key requirement for managing obscured digits and overlapping numbers. The simultaneously precise digit boundary detection capability remains optimal because the approach successfully maintains the clarity of boundaries when digit paths intersect despite ConvLSTM’s [SHI *et al.*, 2015] tendency to disrupt object structures.

The performance of our proposed model was further evaluated on two challenging real-world datasets: KTH Action and CASIA-B. Quantitative results for both datasets are summa-

Model	PSNR \uparrow	SSIM \uparrow	LPIPS \downarrow	MSE \downarrow	Computation Time (s)
PredRNN [Wang <i>et al.</i> , 2017]	18.1	0.88	6.9	75.1	59.00
PredRNN-V2 [Wang <i>et al.</i> , 2022]	17.9	0.879	6.8	74.2	51.50
Eidetic 3D LSTM [Wang <i>et al.</i> , 2019]	17.5	0.749	17	90.1	31.00
MMVP [Zhong <i>et al.</i> , 2023]	15.3	0.802	19.3	89.1	30.10
CrevNet [Yu <i>et al.</i> , 2020]	17	0.76	20	97.8	23.80
LMCNet [Lee <i>et al.</i> , 2021]	17.5	0.76	17.1	92	23.00
PhyDnet [Guen and Thome, 2020]	19.3	0.837	14.8	62.5	20.60
SVG [Denton and Fergus, 2018]	17.7	0.872	8.2	81	19.90
MAU [Chang <i>et al.</i> , 2021]	19.6	0.91	5.98	48	19.80
SAVP [Lee <i>et al.</i> , 2018]	18.2	0.909	6.13	28.61	18.90
SwinLSTM [Tang <i>et al.</i> , 2023]	43.1	0.971	2.8	14.7	18.10
STAU [Chang <i>et al.</i> , 2022]	18.5	0.885	5.3	25.41	16.00
Proposed Model	22.5	0.935	4.8	43.5	14.10

Table 3: Quantitative comparison of video prediction models on the Moving MNIST dataset.

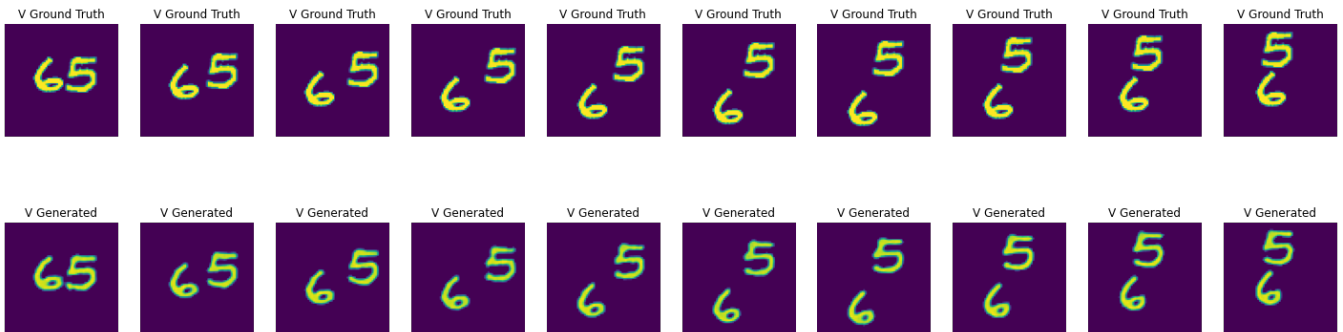


Figure 2: Visual comparison of generated frames of the Moving MNIST dataset.

ized in Table 4 and Table 5, respectively.

4 Comparative Analysis with a Diverse Range of Models

The KTH dataset demands predictions of complex human motions that include walking, boxing and waving actions together with their complex motion structures and temporal relationship patterns. Our model achieves the greatest pixel-level accuracy measured by MSE along with the highest SSIM value compared to MAU and PredRNN. The dynamic spatial temporal fusion mechanism of the MAUCell improves performance due to its ability to identify essential human action features while sustaining frame structural integrity throughout time. The proposed model delivers superior results in PSNR measurements to demonstrate its capability for high-resolution visual frame reconstruction that sustains continuous movement when participants engage in fast motions such as jogging or running. Our model’s pixel-level attention mechanism performs better than PredRNN by delivering refined details throughout brief time frame predictions despite focusing on long-term spatial temporal dependencies. The model’s attention mechanisms operate efficiently by automatically adapting to various motion patterns without depending on explicit hierarchical structure.

The CASIA-B dataset presents unique challenges related to viewpoint variations and occlusions, requiring robust modeling of human gait patterns under diverse conditions. Our model exhibits superior performance in handling viewpoint variations. This is achieved through the spatial attention mechanism in the MAUCell, which ensures that salient gait features are effectively captured regardless of viewpoint changes. By employing pixel-wise attention, the model ensures that fine-grained motion details are preserved, such as subtle gait changes or occluded limb movements, which are often overlooked by baseline models. Its efficient attention-based architecture processes viewpoint variations and occlusions in real time, making it suitable for practical applications in surveillance or gait analysis.

Our proposed MAUCell differs from conventional approaches (such as PredRNN) which need hierarchical frameworks [Kim *et al.*, 2019] or separate treatment of spatial and temporal information by enabling real-time feature fusion between these dimensions maintaining both extensive contextual relationships and detailed pixel data. The method delivers uniform output for multiple motion patterns as well as varied viewpoints. The MAUCell achieves superior performance than SwinLSTM models due to its lightweight structure yet operates with deeper efficiency.

The Moving MNIST dataset underwent ablation studies

Model	PSNR \uparrow	SSIM \uparrow	LPIPS \downarrow	MAE \downarrow	MSE \downarrow
MAU	35.1	0.98	3.57	40.3	0.93
PredRNN-V2	26.85	0.946	5.97	77.7	8.02
SwinLSTM	34.8	0.897	3.22	20.21	6.02
Proposed Model	38.5	0.991	1.97	33.02	0.63

Table 4: Quantitative comparison of video prediction models on the KTH Action dataset.

Model	PSNR \uparrow	SSIM \uparrow	LPIPS \downarrow	MAE \downarrow	MSE \downarrow
MAU	23.04	0.759	23.81	171	19.5
SwinLSTM	20.02	0.521	38.20	291	46.6
Proposed Model	25.24	0.843	21.11	162	13.5

Table 5: Quantitative comparison of video prediction models on the CASIA-B dataset.

to determine individual component effects in our model implementation. Multiple loss function configurations receive analysis in Table 6 including both reconstruction loss and GAN loss and their combined forms.

The model’s potential to improve perception during reconstruction-only training remains constrained due to missing adversarial components thus providing less photorealistic results. The GAN component excels at delivering high perceptual quality but its lack of reconstruction guidance leads predictions away from the original input.

The use of GAN loss with reconstruction loss compounds simulation texture quality as well as pixel-by-pixel precision while demonstrating beneficial impacts of two fundamental loss functions. The absence of an explicit penalties mechanism designed to address structural mismatches creates substandard outputs from the system. A combination between MSE loss for precise structural arrangement and GAN for realistic visual perception maintains optimized results in the full loss approach. Reconstruction loss achieves target alignment between predictions and ground truth while maintaining precise pixel accuracy together with visual quality. The combined operation of these components achieves the optimal performance through their mutual enhancements while emphasizing that integrated loss components create superior outcomes.

Our comparisons included a wide range of models to provide a thorough understanding of our model’s position in the existing landscape of video prediction research:

RNN-based Models To understand our model’s performance we tested it against established versions of ConvLSTM [Wang *et al.*, 2017; Lin *et al.*, 2020], PredRNN [Wang *et al.*, 2017; Wang *et al.*, 2022] and E3D-LSTM [Wang *et al.*, 2019] such as [Shi *et al.*, 2017] a GRU, position based extension of ConvLSTM, etc. Temporal information management within these models relies on distinct memory systems alongside transition approaches. The model achieved superior results than previous models both for short duration and extended range forecasting scenarios.

CNN-based Models The research employed SimVP [Gao *et al.*, 2022] as CNN-based models alongside other methods. The predictive results show meritorious performance metrics

when leaving out recurrent model complexity from the system design. The proposed model performs better than previously tested models when operating under demanding conditions of prediction.

Transformer-based models Research into Transformer-based models centered primarily around the work presented in [Tang *et al.*, 2023] recently emerged. Our model demonstrates that similar resource consumption reveals no significant benefits when compared to these approaches according to studies in [Wang *et al.*, 2017; Tang *et al.*, 2023; Gao *et al.*, 2022].

Stochastic Models This research should explore model trade-offs between deterministic methods by comparing their results against SVG-FP and SVG-LP [Lee *et al.*, 2021; Denton and Fergus, 2018] and VAE-GAN models [Chang *et al.*, 2022; Wang *et al.*, 2017; Denton and Fergus, 2018; Lee *et al.*, 2018]. The models include latent variables as part of their predictive framework to generate diverse possible future scenarios. Anticipating future work it is suggested in [Chang *et al.*, 2021] that our model could benefit from improvement through incorporation of stochastic variations [Babaeizadeh *et al.*, 2018] capability.

5 Conclusion

The proposed model constitutes an essential progression for video prediction through its integration of spatio-temporal attention methods with Generative Adversarial Networks. The model shows superior performance across multiple evaluation metrics and various datasets while achieving better results than current leading approaches for scenarios with overlapping motion and view variation conditions. Through its dynamic approach to spatio-temporal fusion this model produces precise motion modeling between local and global dynamics allowing accurate predictions in all types of environments.

Through its combination of temporal and spatial and pixel-level attention techniques the model learns to pinpoint essential areas within individual frames. The carefully constructed attention system improves the structural integrity of video structures while simultaneously boosting visual quality

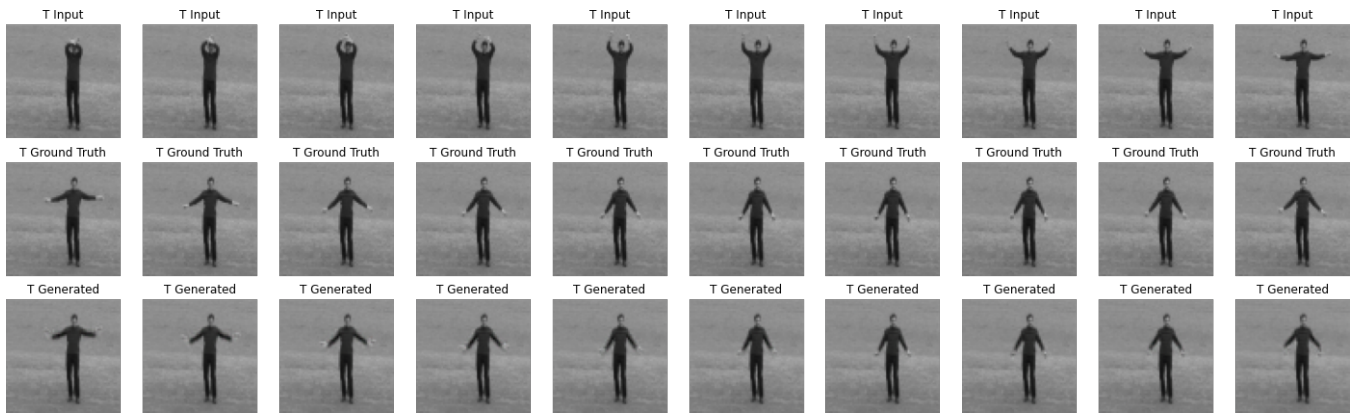


Figure 3: Visual comparison of generated frames of the KTH action dataset.

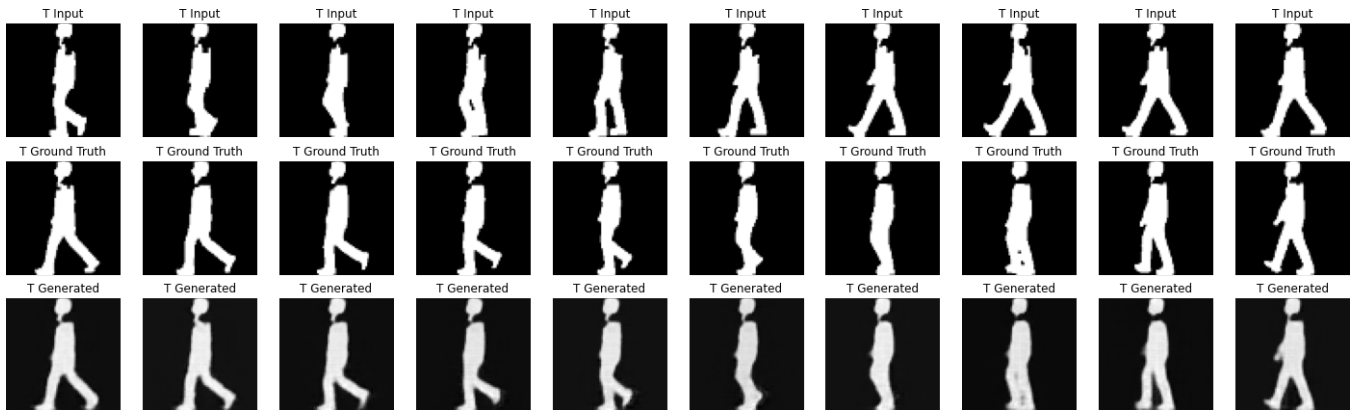


Figure 4: Visual comparison of generated frames of the CASIA-B dataset.

to achieve realistic motion video outputs. The implementation of GAN components produces a significant improvement in realistic image quality within the generated frames. Real-time processing speed for the model reaches 14.1 seconds per sequence which outperforms other methods providing this capability. Its structure and its 79 million parameter base makes it appropriate for resource-limited deployment scenarios.

The existing framework centers its design around deterministically evolving systems. The model delivers successful results on Moving MNIST and KTH Action along with CASIA-B yet needs additional development capabilities for the handling of severe combinations of observational disturbance and angular position modifications during rapid movements.

The development of hybrid models which unite stochastic representations together with spatial-temporal dynamics should be a primary objective for future research to better capture uncertain elements in video sequences. A combination of present-day model architectures should be investigated to reach optimal performance under complex unstructured scenarios. Extended model functionality becomes possible by implementing supplementary information modalities including depth trace and audio and infrared signals for further prediction enhancement.

References

- [Akan *et al.*, 2021] Adil Kaan Akan, Erkut Erdem, Aykut Erdem, and Fatma Güney. Slamp: Stochastic latent appearance and motion prediction, 2021.
- [Babaeizadeh *et al.*, 2018] Mohammad Babaeizadeh, Chelsea Finn, Dumitru Erhan, Roy H. Campbell, and Sergey Levine. Stochastic variational video prediction, 2018.
- [Castro *et al.*, 2016] Francisco Castro, Manuel Marín-Jiménez, and Nicolas Guil. Multimodal features fusion for gait, gender and shoes recognition. *Machine Vision and Applications*, 27, 11 2016.
- [Chang *et al.*, 2021] Zheng Chang, Xinfeng Zhang, Shanshe Wang, Siwei Ma, Yan Ye, Xiang Xinguang, and Wen Gao. Mau: A motion-aware unit for video prediction and beyond. In M. Ranzato, A. Beygelzimer, Y. Dauphin, P.S. Liang, and J. Wortman Vaughan, editors, *Advances in Neural Information Processing Systems*, volume 34, pages 26950–26962. Curran Associates, Inc., 2021.
- [Chang *et al.*, 2022] Zheng Chang, Xinfeng Zhang, Shanshe Wang, Siwei Ma, and Wen Gao. Stau: A spatiotemporal-aware unit for video prediction and beyond, 2022.

Loss	PSNR \uparrow	SSIM \uparrow	LPIPS \downarrow	MAE \downarrow	MSE \downarrow
Reconstruction (L1)	15.7	0.75	16.5	165	91
GAN	13.3	0.62	13.1	243	185
GAN+L1	11.4	0.71	23.2	311	238
GAN+L1+MSE	19.8	0.88	4.7	72	38

Table 6: Ablation studies of the GAN component on the MNIST data.

- [Deng, 2012] Li Deng. The mnist database of handwritten digit images for machine learning research. *IEEE Signal Processing Magazine*, 29(6):141–142, 2012.
- [Denton and Fergus, 2018] Remi Denton and Rob Fergus. Stochastic video generation with a learned prior, 2018.
- [Gao *et al.*, 2022] Zhangyang Gao, Cheng Tan, Lirong Wu, and Stan Z. Li. Simvp: Simpler yet better video prediction, 2022.
- [Guen and Thome, 2020] Vincent Le Guen and Nicolas Thome. Disentangling physical dynamics from unknown factors for unsupervised video prediction, 2020.
- [Izaak Neutelings,] Izaak Neutelings. Neural networks. https://tikz.net/neural_networks/.
- [Kim *et al.*, 2019] Taesup Kim, Sungjin Ahn, and Yoshua Bengio. Variational temporal abstraction. In H. Wallach, H. Larochelle, A. Beygelzimer, F. d'Alché-Buc, E. Fox, and R. Garnett, editors, *Advances in Neural Information Processing Systems*, volume 32. Curran Associates, Inc., 2019.
- [Kwon and Park, 2019] Yong Hoon Kwon and M. Park. Predicting future frames using retrospective cycle gan. *2019 IEEE/CVF Conference on Computer Vision and Pattern Recognition (CVPR)*, pages 1811–1820, 2019.
- [Lee *et al.*, 2018] Alex X. Lee, Richard Zhang, Frederik Ebert, Pieter Abbeel, Chelsea Finn, and Sergey Levine. Stochastic adversarial video prediction, 2018.
- [Lee *et al.*, 2019] Jungbeom Lee, Jangho Lee, Sungmin Lee, and Sungroh Yoon. Mutual suppression network for video prediction using disentangled features, 2019.
- [Lee *et al.*, 2021] Sangmin Lee, Hak Gu Kim, Dae Hwi Choi, Hyung-Il Kim, and Yong Man Ro. Video prediction recalling long-term motion context via memory alignment learning, 2021.
- [Lin *et al.*, 2020] Zihui Lin, Maomao Li, Zhuobin Zheng, Yangyang Cheng, and Chun Yuan. Self-attention convlstm for spatiotemporal prediction. *Proceedings of the AAAI Conference on Artificial Intelligence*, 34:11531–11538, 04 2020.
- [Michalski *et al.*, 2014] Vincent Michalski, Roland Memisevic, and Kishore Konda. Modeling deep temporal dependencies with recurrent grammar cells. In Z. Ghahramani, M. Welling, C. Cortes, N. Lawrence, and K.Q. Weinberger, editors, *Advances in Neural Information Processing Systems*, volume 27. Curran Associates, Inc., 2014.
- [Riebesell and Bringuier, 2022] Janosh Riebesell and Stefan Bringuier. Scientific Diagrams, December 2022.
- [Schuldt *et al.*, 2004] C. Schuldt, I. Laptev, and B. Caputo. Recognizing human actions: a local svm approach. In *Proceedings of the 17th International Conference on Pattern Recognition, 2004. ICPR 2004.*, volume 3, pages 32–36 Vol.3, 2004.
- [SHI *et al.*, 2015] Xingjian SHI, Zhourong Chen, Hao Wang, Dit-Yan Yeung, Wai-kin Wong, and Wang-chun WOO. Convolutional lstm network: A machine learning approach for precipitation nowcasting. In C. Cortes, N. Lawrence, D. Lee, M. Sugiyama, and R. Garnett, editors, *Advances in Neural Information Processing Systems*, volume 28. Curran Associates, Inc., 2015.
- [Shi *et al.*, 2017] Xingjian Shi, Zhihan Gao, Leonard Lausen, Hao Wang, Dit-Yan Yeung, Wai kin Wong, and Wang chun Woo. Deep learning for precipitation nowcasting: A benchmark and a new model, 2017.
- [Srivastava *et al.*, 2016] Nitish Srivastava, Elman Mansimov, and Ruslan Salakhutdinov. Unsupervised learning of video representations using lstms, 2016.
- [Sun *et al.*, 2023] Mingzhe Sun, Weining Wang, Xinxin Zhu, and Jing Liu. Moso: Decomposing motion, scene and object for video prediction. *2023 IEEE/CVF Conference on Computer Vision and Pattern Recognition (CVPR)*, pages 18727–18737, 2023.
- [Tang *et al.*, 2023] Song Tang, Chuang Li, Pu Zhang, and RongNian Tang. Swinlstm:improving spatiotemporal prediction accuracy using swin transformer and lstm, 2023.
- [Villar-Corrales *et al.*, 2022] Angel Villar-Corrales, Ani Karapetyan, Andreas Boltres, and Sven Behnke. Msprede: Video prediction at multiple spatio-temporal scales with hierarchical recurrent networks, 2022.
- [Villegas *et al.*, 2019] Ruben Villegas, Arkanath Pathak, Harini Kannan, Dumitru Erhan, Quoc V. Le, and Honglak Lee. High fidelity video prediction with large stochastic recurrent neural networks, 2019.
- [Wang *et al.*, 2017] Yunbo Wang, Mingsheng Long, Jianmin Wang, Zhifeng Gao, and Philip S Yu. Predrnn: Recurrent neural networks for predictive learning using spatiotemporal lstms. In I. Guyon, U. Von Luxburg, S. Bengio, H. Wallach, R. Fergus, S. Vishwanathan, and R. Garnett, editors, *Advances in Neural Information Processing Systems*, volume 30. Curran Associates, Inc., 2017.
- [Wang *et al.*, 2018] Yunbo Wang, Zhifeng Gao, Mingsheng Long, Jianmin Wang, and Philip S. Yu. Predrnn++: Towards a resolution of the deep-in-time dilemma in spatiotemporal predictive learning, 2018.

- [Wang *et al.*, 2019] Yunbo Wang, Lu Jiang, Ming-Hsuan Yang, Li-Jia Li, Mingsheng Long, and Li Fei-Fei. Eideitic 3d LSTM: A model for video prediction and beyond. In *International Conference on Learning Representations*, 2019.
- [Wang *et al.*, 2022] Yunbo Wang, Haixu Wu, Jianjin Zhang, Zhifeng Gao, Jianmin Wang, Philip S. Yu, and Mingsheng Long. Predrnn: A recurrent neural network for spatiotemporal predictive learning, 2022.
- [Yee Andres,] Yee Andres. CASIA-B pretrated. <https://www.kaggle.com/datasets/yeeandres/casiabpretreated>.
- [Yu *et al.*, 2020] Wei Yu, Yichao Lu, Steve Easterbrook, and Sanja Fidler. Efficient and information-preserving future frame prediction and beyond. In *International Conference on Learning Representations*, 2020.
- [Zhong *et al.*, 2023] Yiqi Zhong, Luming Liang, Ilya Zharkov, and Ulrich Neumann. Mmvp: Motion-matrix-based video prediction, 2023.

A Appendix

A.1 Hardware Specification

System Processor	AMD Ryzen Threadripper 3960X 24-Core Processor @ 3.8Ghz
Graphics	GeForce RTX 3090 with 24 GB RAM
System Memory	64 GB Ram

Table 7: System Hardware